A Novel Transmission Scanner Framework for Real-Time Applications

Dirk Kolb[1,2]**, Ulla Uebler**[1]**, Elmar Nöth**[2]
1 - MEDAV GmbH, Gräfenberger Str. 32-34, 91080 Uttenreuth, Germany
2 - Pattern Recognition Lab, Department of Computer Science, Friedrich-Alexander-University Erlangen-Nuremberg, Martensstr. 3, 91058 Erlangen, Germany
dirk.kolb@medav.de, ulla.uebler@medav.de, noeth@informatik.uni-erlangen.de

ABSTRACT

The strong need for a robust and real-time transmission classification can be found both in civil and non-civil applications. In this paper, we propose a new technique based on modern low- and high-complexity object detection approaches. The transmission scanner uses a combination of Haar-like and technical features to detect and classify different, co-occurring narrowband transmissions within wideband signals. The transmission scanner is evaluated with recorded real world data in order to fulfill real conditions. The evaluation shows that this system performs very well with 99.5% accuracy.

1.0 INTRODUCTION

To know what is on air has always been a strong interest of civil and non-civil institutions. The civil area of research has the aim to detect white spaces in frequency bands in order to establish secondary usage, as it is done in Cognitive Radio (CR) [1, 2]. In contrast to this, the non-civil institutions try to identify every signal or a special type of signal. This signal interception is called Communications Intelligence (COMINT). Both benefit from increasing instantaneous receiver bandwidths, made possible by Software-Defined Radio (SDR) [3]. The wider the bandwidth, the higher the knowledge gain can be. The drawback of such a wideband receiver is that the requirements for a real-time signal processing in CR and COMINT applications are higher than before, as the search space increases.

In Fig. 1 a traditional procedural method is shown, which is often applied in COMINT applications. A Wideband Receiver (WBR) digitizes the antenna signal with a specific sampling frequency. The typical sampling frequencies for the High Frequency (HF), Very and Ultra High Frequency (VUHF) bands vary between $f_S = 625$ kHz and $f_S = 20$ MHz. The discretized signal is led to a Wideband Signal Detection (WDET). Most of the approaches for this stage are based on an energy detection. A priori knowledge is not used to extract the information regarding the center frequency, bandwidth, transmission start and duration. The resulting information of WDET is used within the Digital Down Conversion (DDC) to cut the narrowband signals out of the wideband signal and transfer them to the Narrowband Transmission Classification (NTCL). The NTCL extracts specific features, e. g., modulation type and baud rate, in order the get the information about the used transmission standard, e. g., STANAG-4285 or PACTOR II [4], which can be found in the High Frequency (HF) between 3 MHz and 30 MHz. Approaches for the modulation classifier are presented in [5–8]. The evaluation of most of these algorithms was done without consideration of inaccuracies of the

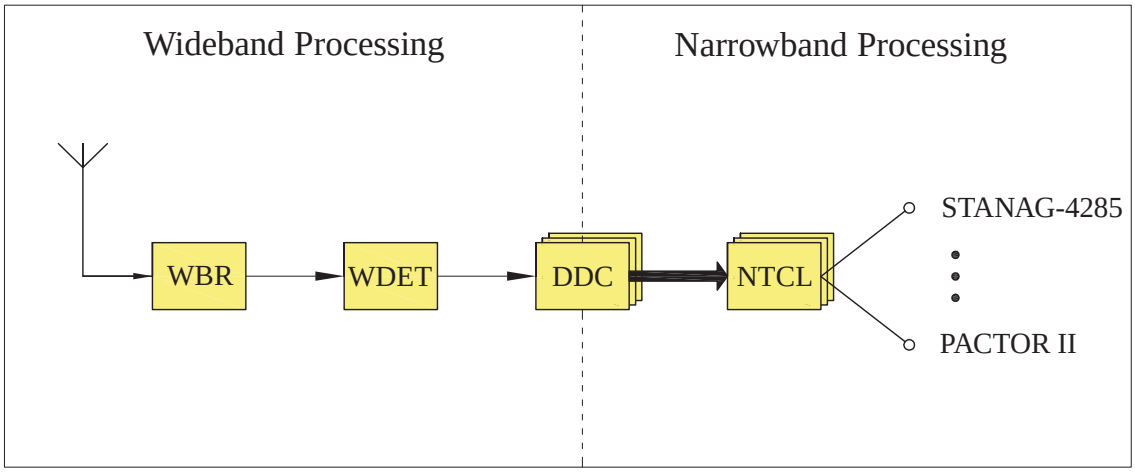

Figure 1: Processing chain with separated wideband signal detection and narrowband transmission classification.

first stage and furthermore almost all test signals were created without consideration of transmission standards. Therefore, two problems arise in real applications. First, most of the classification approaches used in NTCL extract features or technical parameters which loose their quality in case of detection inaccuracies, e. g., frequency offset. Second, some technical parameters, especially the modulation type, are unambiguous: a STANAG-4285 transmission changes the modulation type periodically and a PACKET-RADIO [4] transmission is additionally frequency modulated in the VUHF bands. Therefore, a feature, which is able to distinguish specific modulation types, might fail in applications where a signal with different modulation types commonly occurs. Another problem, as shown in the block diagram in Fig. 1, is the separation of wideband and narrowband processing. The resulting quality of WDET degrades in case of lower signal-to-noise ratios (SNRs) or stronger fading effects. This leads to incorrect information for the DDC block and to useless narrowband signals for the NTCL stage. In most of the cases the classification results are incorrect. Thus, it is advisable to avoid a separation between wideband and narrowband processing or to combine signal detection and classification.

With tremendously increased processing power, more research was done in SDR and CR. Both CR and SDR gained importance in civil projects, e. g. the reorganization of public safety communications or the establishment of Wireless Regional Area Networks (WRANs) in rural environments [9]. With this ongoing development new strategies of an improved combined detection and classification emerged. Beside the typical energy based detectors [10] the first detectors using a priori knowledge came up. These detectors are based on features, for example, second-order cyclostationarity [11, 12] or autocorrelation [13]. They are reliable even at very low SNR values, but the computational effort is very high. Within the presented literature it is mostly assumed that the center frequencies of the signals of interest are well known, which is true for most so-called cooperative applications. In non-civil or non-cooperative applications the only assumption that can be made is that there might be a signal of interest at an unknown position. This requires a scanning classification system which is possible to perform the scanning and classification process in real-time.

In this paper we combine the knowledge from the COMINT background with new techniques from CR and modern pattern recognition approaches. We present a flexible combined transmission detection and classification for both cooperative and non-cooperative applications. It will be trained for a common HF

transmission standard. The system is evaluated with real signals in order to show the robustness.

The paper is organized as follows: Section 2.0 describes the principle of transmission scanning. In Section 2.1, we present the features used for the classification. Section 2.2 analyzes the classification system. Section 3.0 reports on the performance of our system. In Section 4.0, we present conclusions along with recommendations for future improvements.

2.0 TRANSMISSION SCANNER FRAMEWORK

The basis of our approach is the spectrogram of a wideband signal. In Fig. 2 only a small part of a wideband spectrogram is shown. Many experts are able to detect and classify transmissions only by looking at this special visualization. Thus, the principle of our proposed transmission scanner is comparable to well-known object detection techniques (e. g., face detection [14]), which are applied to images. In short, the scan is a series of detections and classifications of different masks which are moved over the image. In our case, the image is comparable with the complex spectrogram $\mathbf{X}$

$$\mathbf{X} = \begin{bmatrix} \mathbf{x}_1 \\ \vdots \\ \mathbf{x}_i \\ \vdots \\ \mathbf{x}_{t_\mathrm{N}} \end{bmatrix} = \begin{bmatrix} X\left[1,1\right] & \dots & X\left[1,j\right] & \dots & X\left[1,f_\mathrm{FFT}\right] \\ \vdots & \ddots & \vdots & & \\ X\left[i,1\right] & \dots & X\left[i,j\right] & \dots & X\left[i,f_\mathrm{FFT}\right] \\ \vdots & & \vdots & \ddots & \\ X\left[t_\mathrm{N},1\right] & \dots & X\left[t_\mathrm{N},j\right] & \dots & X\left[t_\mathrm{N},f_\mathrm{FFT}\right] \end{bmatrix}, \tag{1}$$

where $|\mathbf{x}_i|$ are the bins of the power spectrum and t_N is the number of short-time spectrums used for classification. $\mathbf{x}_i$ is computed within the wideband receiver, a ComCat$^{\mathrm{TM}}$-Tuner, delivered by MEDAV [15]. With an applied FFT length $f_\mathrm{FFT} = 4096$ samples, a sampling frequency $f_S = 625$ kHz and a Hann window with 50% overlapping, we receive a frequency resolution $\Delta f = 153$ Hz and a time resolution $\Delta t = 0.003$ sec[1]. The mentioned mask is fitted to the transmission we are looking for. In Section 3.0 the transmission of interest is a STANAG-4285 signal. It is a continuous, fixed frequency and about 3.0 kHz wide signal. It became evident that 0.500 s signal length is sufficient for a robust classification. Thus, the mask is 3.3 kHz wide and 0.500 sec long. Lower time lengths are possible, but will result in a lower classification rate. This leads to a mask $\mathbf{X}_\mathrm{M}$, $f_\mathrm{M} = 22$ bins wide and $t_\mathrm{M} = 168$ bins long,

$$\mathbf{X}_\mathrm{M}\left(u,v\right) = \begin{bmatrix} X\left[u,v\right] & \dots & X\left[u,v+f_\mathrm{M}\right] \\ \vdots & \ddots & \vdots \\ X\left[u+t_\mathrm{M},v\right] & \dots & X\left[u+t_\mathrm{M},v+f_\mathrm{M}\right] \end{bmatrix}, \tag{2}$$

where $u = [1, ..., t_\mathrm{N} - t_\mathrm{M}]$ is the position in time direction and $v = [1, ..., f_\mathrm{FFT} - f_\mathrm{M}]$ the position in frequency direction of $\mathbf{X}$. In Fig. 3 the block diagram for the new system is shown. By sweeping of $\mathbf{X}_\mathrm{M}$ or rather varying u and v, all possible mask positions within $\mathbf{X}$ are sent to the wideband feature extraction and then to the wideband classification. The wideband feature extraction is described in Section 2.1 and the wideband classification in Section 2.2.

[1]These resolutions are adapted to the HF range. For the VUHF bands other resolutions should be chosen.

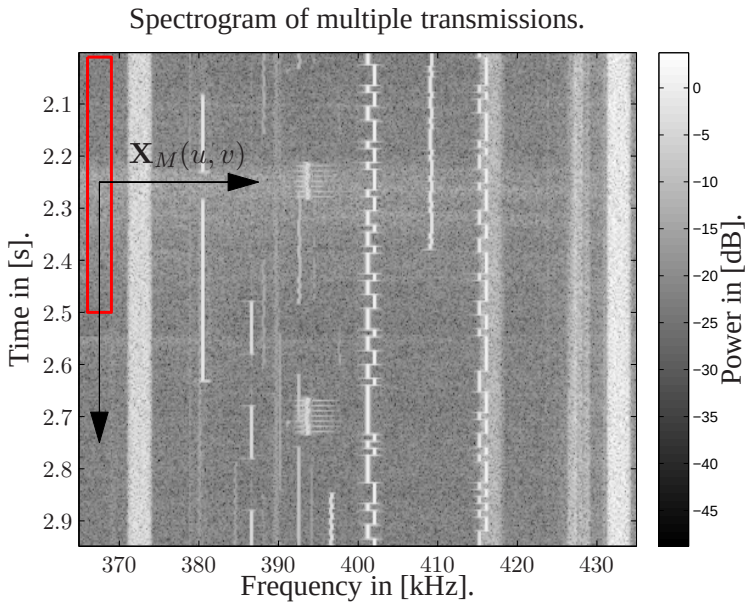

(a)

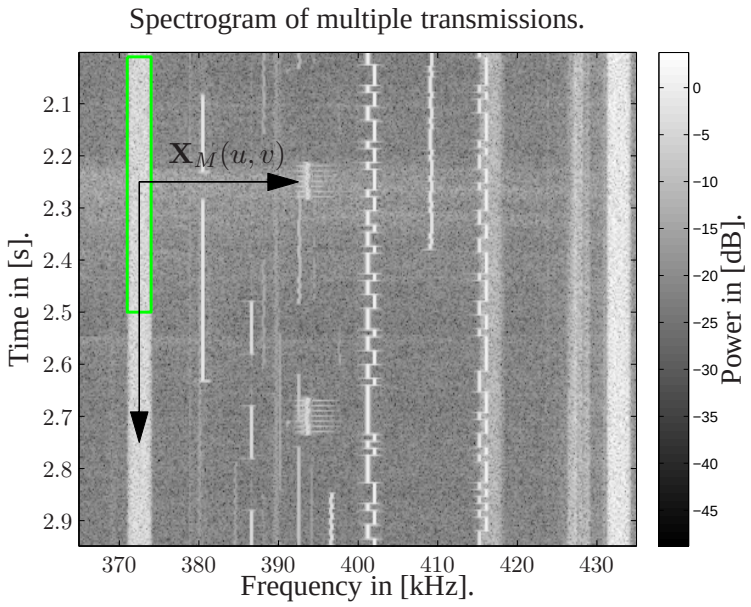

(b)

Figure 2: Part of an absolute, logarithmic wideband spectrogram. It contains several transmissions, for example, STANAG-4285 and BAUDOT. A STANAG-4285 mask $\mathbf{X}_M$ with $f_M = 22$ bins and $t_M = 168$ bins is exemplarily swept over the spectrogram. In Fig. 2(a) $\mathbf{X}_M$ lies not on a STANAG-4285 transmission. In Fig. 2(b) $\mathbf{X}_M$ lies on a STANAG-4285 transmission.

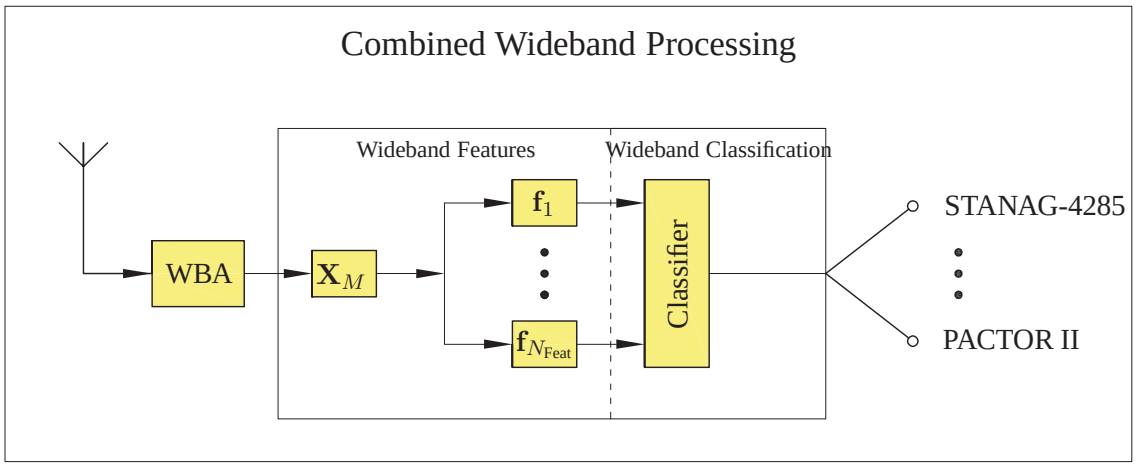

Figure 3: Processing chain with a combined wideband signal detection and transmission classification.

2.1 Wideband Features

For transmission classification, it is desirable to define N_{Feat} different feature types. There are features which are very efficient but not definite, and there are features which allow exact decisions but are very inefficient. Thus, the proposed framework gives us the possibility to include different feature groups and to benefit from the different advantages. At the end of the feature extraction, we obtain a feature vector $\mathbf{f}$

$$\mathbf{f} = [\mathbf{f}_1, \ldots, \mathbf{f}_{N_{\text{Feat}}}] \tag{3}$$

with N

$$N = N_1 + \ldots + N_{N_{\text{Feat}}} \tag{4}$$

dimensions.

In the research area of object detection optical features, like Haar-like features, are state of the art. They are very efficient and obtain a good quality. In our approach, we apply the Haar-like features to the logarithmic, absolute mask $\mathbf{X}_{\text{M,log}}$

$$\mathbf{X}_{\text{M,log}} = 10 \cdot \log_{10}\left(|\mathbf{X}_{\text{M}}|^2\right). \tag{5}$$

The original, complex mask $\mathbf{X}_{\text{M}}$ gives us the possibility to extract more information, which is invisible in the logarithmic, absolute spectrogram. In addition to the optical Haar-like features, we use technical, phase-related features, too.

2.1.1 Haar-like Features

The evaluation of every single bin within the mask does not give any information other than signal power and phase information, which is not sufficient for the classification process. So, first of all we need features that encode the relation of different signal power values within one observed mask $\mathbf{X}_{\mathrm{M,log}}$. Haar-like features are typically used to describe contrasts within images. Applied to our problem, these features characterize the two-dimensional energy distribution.

Our Haar-like feature set, which is shown in Fig. 4, was inspired by Papageorgiou *et al.* in [16]. We reduced the number of Haar-like features to a radio signal specific set. It contains now 20 2-D windows, and can be used for different transmission types. Depending on the Haar-like feature, which is used for extraction, different tasks can be fulfilled. Fig. 4(f) and Fig. 4(g) are for the symbol alternations of a 2-FSK transmission, whereas Fig. 4(h) is useful for the bandwidth estimation.

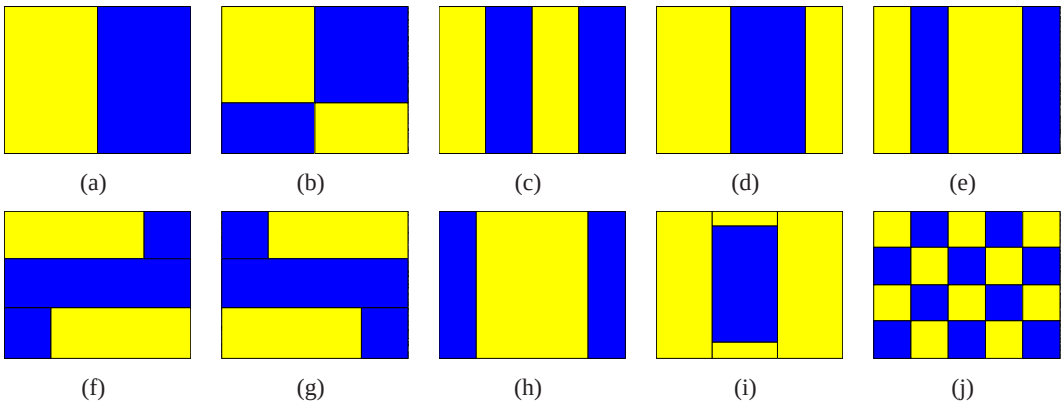

Figure 4: Haar-like features used for detection and classification. Dark-colored areas have negative and light-colored areas positive weights.

The Haar-like features are applied to different positions with variable scale factors within the mask $\mathbf{X}_{\mathrm{M}}$, as it is shown in Fig. 5. In this case, the resulting feature value is the difference between the rectangle A and rectangle B. Considering all possible positions and scaling factors, $N_{\mathrm{Haar}} = 362.720$ Haar-like features are extracted. Viola *et al.* showed in [14] a very fast computation scheme based on integral images, which was adapted in our implementation.

2.1.2 Phase-related Feature

In this paper we introduce a new technical feature which is especially suited to detect periodic sequences within a transmission. These sequences are part of a standard and often used, to enable equalization algorithms, like it is done within the STANAG-4285 standard, or to avoid interference among transmissions in Orthogonal Frequency-Division Multiplexing (OFDM) communications. The proposed feature is based on a cepstral analysis, which is suitable for the detection of periodic values, as described by Bogert *et al.* in [17]. Similar to the cyclostationary feature, presented by Gardner *et al.* in [11], the cepstral feature is modulation type independent. Thus, it is suitable for transmissions with changing modulation types or some double modulated content. The distance between training sequences is generally unique for different transmission

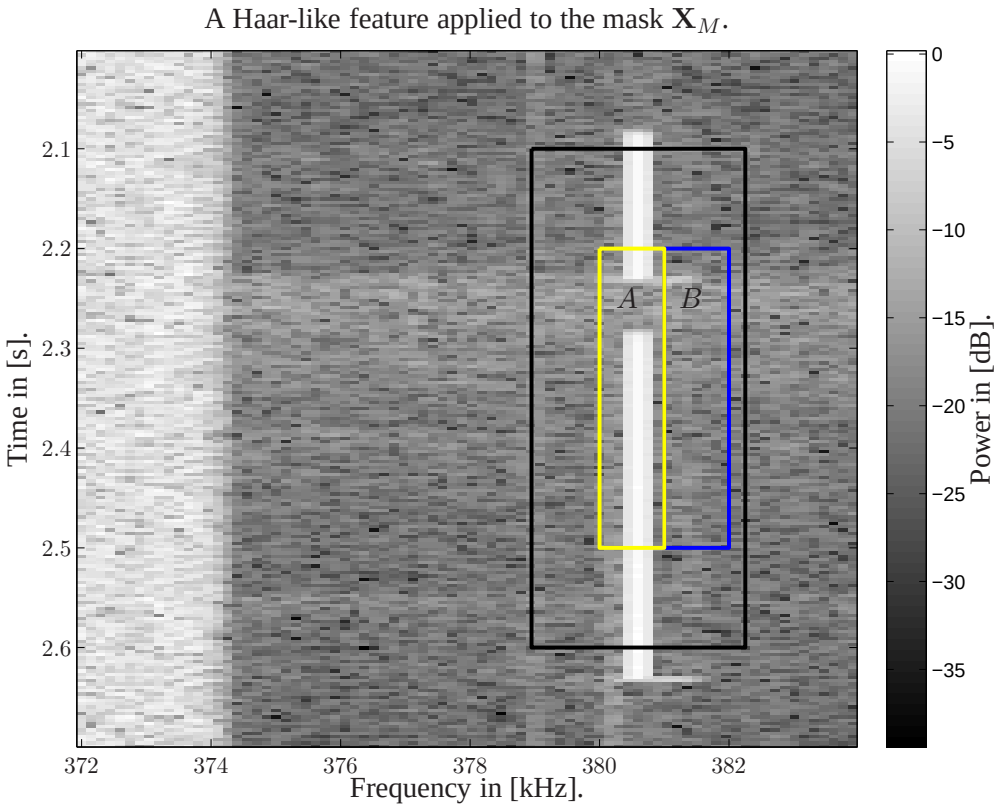

Figure 5: The Haar-like feature, which is shown in Fig. 4(a), is applied to the mask $\mathbf{X}_M$ at a certain position and with specific scaling factors.

standards. The cepstrum $q_{\text{Ceps}}(t)$ of a complex signal $q(t)$ can be expressed as a function, as follows

$$q_{\text{Ceps}}(t) = \left| \int_{-\infty}^{+\infty} \log\left(\left| Q(w)^2 \right| \right) e^{-jwt} dw \right|^2, \tag{6}$$

where $Q(w)$ is

$$Q(w) = \int_{-\infty}^{+\infty} q(t)\, e^{-jwt} dt. \tag{7}$$

In our case, $q(t)$ is the downsampled narrowband signal, dependent on the position of the mask $\mathbf{X}_{\text{M}}$ within $\mathbf{X}$. In Fig. 6 the cepstrum of two transmissions is plotted. It shows the position of a training sequence and its harmonics. Exploiting the harmonic structure within the cepstrum, the distance between the sequences can be extracted and used for classification. In both cases a peak analysis gives the correct result of 106.6 msec between the sequences. In Fig. 6(b) it emerged that the cepstrum is very robust against fading and low SNR. With $N_{\text{Cepst}} = 1$ and according to (3), we obtain a feature vector $\mathbf{f}$ with $N = 362.721$ different elements.

2.2 Wideband Classifier

Given a set of labeled feature vectors, which are computed from the signal and rejection patterns, any machine learning approach can be used to learn a functional relationship between feature values and classes.

Although the Haar-like features can be computed very efficiently, extracting the complete set is very expensive. So, we decided to use the Adaptive Boosting (AdaBoost) algorithm, which is well-known in object detection and first published by Freund *et al.* in [18]. AdaBoost trains T weak classifiers $h_t(\mathbf{X}_\mathrm{M})$ repeatedly with $t = 1, \ldots, T$. The final strong classifier is a weighted combination of the iterated hypotheses h_t. Generally, for every iteration a weak classifier which evaluates a threshold Θ_t on a single feature f_t is trained to distinguish between the signal class c_1 and the rejection class c_2:

$$h_t(\mathbf{X}_\mathrm{M}) = \begin{cases} c_1, & f_t(\mathbf{X}_\mathrm{M}) < \Theta_t \\ c_2, & \text{otherwise} \end{cases} \tag{8}$$

After each iteration, the training set is reweighted with respect to the error rate of the last weak classifier. As T is chosen to be smaller than the overall number of available features N, the number of features will be reduced during the training process. N' will remain after the training:

$$N' << N \;\text{ with }\; N' = N'_\mathrm{Haar} + N'_\mathrm{Cepst}. \tag{9}$$

It can happen that N'_Haar or N'_Cepst is zero. In this case the corresponding feature group will not be used for the classification process. For more details regarding AdaBoost, see [18].

3.0 EXPERIMENTAL RESULTS

The task is to detect STANAG-4285 transmissions in wideband signals without prior knowledge, e. g., the exact position, and reject noise and all other transmissions. For the experiments, we trained three different, monolithic AdaBoost classifiers with $T = 10$ weak classifiers. The first classifier is trained with both feature groups $\mathbf{f}_\mathrm{Haar}$ and $\mathbf{f}_\mathrm{Ceps}$, while the others are trained each with feature group $\mathbf{f}_\mathrm{Haar}$ or $\mathbf{f}_\mathrm{Ceps}$.

Unfortunately, there exists no realistic labeled data from real world transmissions. Thus, the wideband signals used for this work were acquired and manually labeled by MEDAV. Researchers, interested in a comparison with their own approach, can have access to the data upon request. The wideband signal for training has a sampling frequency $f_s = 625$ kHz and a center frequency $f_c = 8.350$ MHz. The wideband signal for the evaluation has the same sampling frequency but a center frequency of $f_c = 8.800$ MHz. To provide typical rejection samples for this scenario, the rejection class contains examples of noise and examples of common HF transmissions, e. g., SITOR-ARQ, BAUDOT, GW-PACTOR, GW-OFDM, J3E-USB and A1E (described by Prösch in [4]). The used wideband signals are an important part of the realistic evaluation, as they represent a typical HF scenario. They contain a lot of unknown transmissions and time-variant wideband noise. In Table 1 the class distribution is shown.

Table 2 shows the results of the evaluation. Compared to the trainings with only one feature group, we obtained the best classification rate of 99.5% for real world scenarios with the combination of $\mathbf{f}_\mathrm{Haar}$ and $\mathbf{f}_\mathrm{Ceps}$. In Fig. 7, only a part of the results is plotted.

The total positive rate for the rejection class is about 99.7%, and the total positive rate for the signal class is 96.3%. This indicates the fact that the combination of both groups is necessary for a robust classification. A high accuracy for the rejection class is highly appreciated in COMINT applications, because the post processing of miss-classified signals is very expensive.

Class	Name	Training	Test
c_1	STANAG-4285	4887	1581
c_2	NOISE	12434	4646
c_2	SITOR-ARQ	2898	2844
c_2	GW-PACTOR	13386	6960
c_2	BAUDOT	5544	6336
c_2	GW-OFDM	9504	5244
c_2	J3E-USB	2088	7032
c_2	A1E	8730	0

Table 1: Number of patterns for training and test set. Due to the realistic properties of the wideband signals, it is possible that some classes have more or less samples, e. g., A1E. Both training and test set contain transmissions with a SNR between 7 dB and 30 dB.

Training and evaluation for $T = 10$					
Feature vector $[\mathbf{f}_{\text{Haar}}, \mathbf{f}_{\text{Ceps}}]$	TP Rate	FP Rate	Precision	Recall	F-Measure
c_1 = STANAG-4285	0.963	0.003	0.932	0.963	0.947
c_2 = REJECTION	0.997	0.037	0.998	0.997	0.997
Weighted Avg.	0.995	0.035	0.995	0.995	0.995
Feature vector $[\mathbf{f}_{\text{Haar}}]$					
c_1 = STANAG-4285	0.822	0.019	0.671	0.822	0.738
c_2 = REJECTION	0.981	0.178	0.991	0.981	0.986
Weighted Avg.	0.973	0.171	0.977	0.973	0.975
Feature vector $[\mathbf{f}_{\text{Ceps}}]$					
c_1 = STANAG-4285	0.917	0.015	0.745	0.917	0.822
c_2 = REJECTION	0.985	0.083	0.996	0.985	0.990
Weighted Avg.	0.982	0.080	0.985	0.982	0.983

Table 2: Evaluation of the classifiers with real world signals. All possible combinations of the feature groups $\mathbf{f}_{\text{Haar}}$ and $\mathbf{f}_{\text{Ceps}}$ were considered.

Using the integral feature computation and some other optimizations, we could greatly reduce the overall complexity. We were able to run about 13.108 classifications per second[2], which is a great step to real-time CR and COMINT applications.

4.0 SUMMARY AND OUTLOOK

The paper introduced a novel method for transmission scanning based on well-established object detection techniques and new CR approaches. In order to improve the accuracy we used beside the typical Haar-like features, also a new cepstral feature. A combination of both feature groups exploited the particular benefits. With signal recordings provided by MEDAV, we could show that our system is capable of handling difficult scenarios, in which different transmission standards and types of fading appear. We obtained very good results for a common, real HF scenario.

[2] A single threaded implementation ran on a Intel®Core™2 Duo CPU T8300 at 2.40 GHz.

As future work, one important issue is to build an efficient multiclass version of the proposed transmission scanner, based on feature sharing. New features, e.g. the correlation-based feature, shown in [13], will be added to the framework. In order to demonstrate the flexibility and the real-time capabilities of our system, we will focus on VUHF transmission standards and scenarios. This step will allow the framework to be used as a monitoring system within CR applications, e.g. the robust emergency or disaster communication systems.

REFERENCES

[1] Mitola III, J. and Maguire, Jr., G., "Cognitive Radio: Making Software Radios More Personal," *Personal Communications, IEEE*, Vol. 6, No. 4, Aug 1999, pp. 13–18.

[2] Mitola III, J., "Cognitive Radio for Flexible Mobile Multimedia Communications." *MONET*, Vol. 6, No. 5, 2001, pp. 435–441.

[3] Mitola III, J., ""Software Radios: Survey, Critical Evaluation and Future Directions"," *Aerospace and Electronic Systems Magazine, IEEE*, Vol. 8, No. 4, Apr 1993, pp. 25–36.

[4] Prösch, R., *Technical Handbook For Radio Monitoring I.*, Book on Demand GmbH, 1st ed., 2007.

[5] Azzouz, E. and Nandi, A., *Automatic Modulation Recognition of Communication Signals*, Kluwer Academic Publishers, 1996.

[6] Fargues, M. and Hatzichristos, G., "A Hierarchical Approach to the Classifiaction of Digital Modulations in Multipath Environments," Tech. rep., Department of Electrical and Computer Engineering, May 2001, NPS-EC-01-004.

[7] Wikström, M., "A Survey of Modulation Classification Methods for QAM Signals," Tech. rep., Command and Control Systems, 2005.

[8] Dobre, O., Abdi, A., Bar-Ness, Y., and Su, W., "A Survey of Automatic Modulation Classification Techniques: Classical Approaches and New Trends," *IET Communications*, Vol. 1, 2007, pp. 137–156.

[9] Cordeiro, C., Challapali, K., Birru, D., and Sai Shankar, N., "IEEE 802.22: The First Worldwide Wireless Standard Based on Cognitive Radios," *New Frontiers in Dynamic Spectrum Access Networks, 2005. DySPAN 2005. 2005 First IEEE International Symposium on*, 8-11 2005, pp. 328 –337.

[10] Digham, F., Alouini, M., and Simon, M., "On the Energy Detection of Unknown Signals Over Fading Channels," *IEEE Transactions on Communications*, Vol. 55, No. 1, 2007.

[11] Gardner, W. and Spooner, C., "Cyclic Spectral Analysis for Signal Detection and Modulation Recognition," *Military Communications Conference, 1988. MILCOM 88, Conference record. '21st Century Military Communications - What's Possible?'. 1988 IEEE*, Vol. 2, Oct 1988, pp. 419–424.

[12] Gardner, W., "Exploitation of Spectral Redundancy in Cyclostationary Signals," *Signal Processing Magazine, IEEE*, Vol. 8, No. 2, Apr 1991, pp. 14–36.

[13] Pérez-Neira, A. I., Lagunas, M. A., Rojas, M. A., and Stoica, P., "Correlation Matching Approach for Spectrum Sensing in Open Spectrum Communications," *Trans. Sig. Proc.*, Vol. 57, No. 12, 2009, pp. 4823–4836.

[14] Viola, P. and Jones, M., "Robust Real-Time Face Detection." *Int. J. Comput. Vision*, Vol. 57, No. 2, 2004, pp. 137–154.

[15] MEDAV GmbH, "ComCat™-Tuner - CCT-NG," 2006.

[16] Papageorgiou, C., Oren, M., and Poggio, T., "A General Framework for Object Detection," *ICCV*, 1998, pp. 555–562.

[17] Bogert, B., Healy, M., and Tukey, J., "The Frequency Analysis of Time Series for Echoes: cepstrum, pseudo-Autocovariance, Cross-Cepstrum, and saphe cracking," *Proc. Symp. Time Series Analysis, Ed.: M. Rosenblatt,John Wiley*, 1963, pp. 209–243.

[18] Freund and Schapire, "A Decision-Theoretic Generalization of On-Line Learning and an Application to Boosting." *JCSS: Journal of Computer and System Sciences*, Vol. 55, 1997.

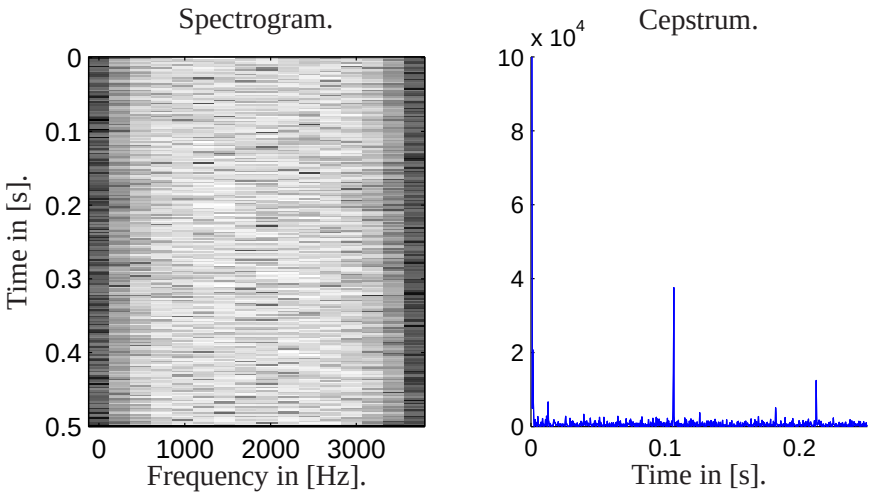

(a)

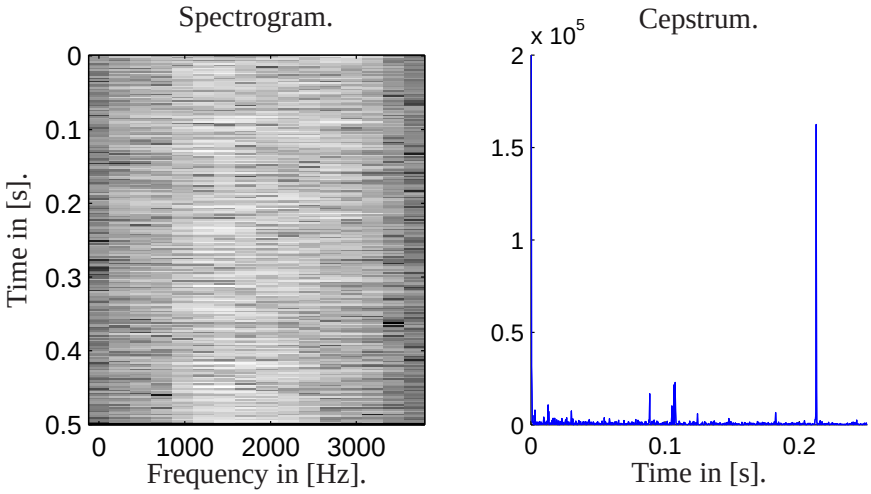

(b)

Figure 6: Spectrograms and cepstra of both a high SNR and a low SNR STANAG-4285 transmission. The dimensions of the spectrogram are equivalent to the dimensions of $\mathbf{X}_M$.

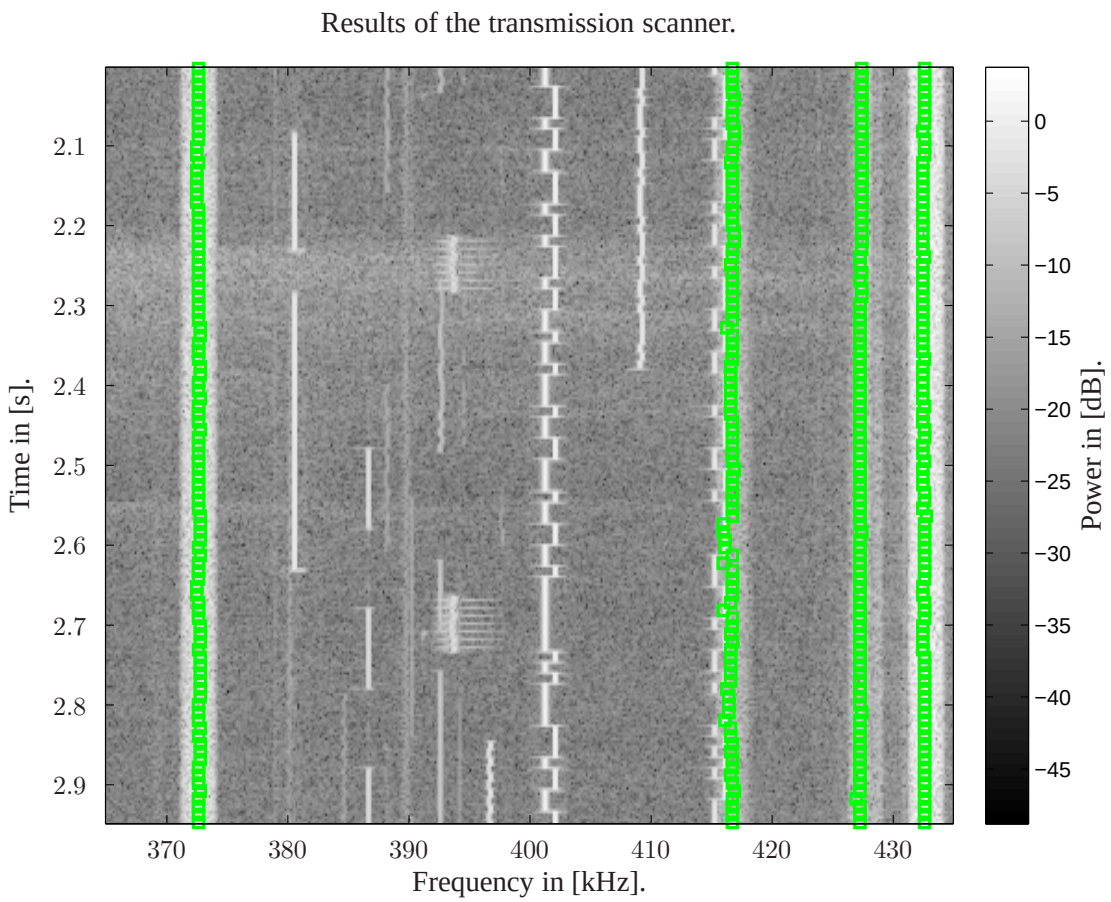

Figure 7: Part of an absolute, logarithmic wideband spectrogram. It contains the results of the transmission scanner, marked as green boxes. This classifier was trained with a combination of f_{Haar} and f_{Ceps}. Every STANAG-4285 transmission was tagged. There is no incorrect hit in this part of the wideband spectrogram.